Materials Letters 203 (2017) 42–45

Contents lists available at ScienceDirect

Materials Letters

journal homepage: www.elsevier.com/locate/mlblue

Temperature effects on formation of carbon-based nanomaterials from kraft lignin

Xuefeng Zhang [a], Qiangu Yan [a], El Barbary Hassan [a], Jinghao Li [b], Zhiyong Cai [b,*], Jilei Zhang [a,*]

[a] Department of Sustainable Bioproducts, Mississippi State University, Mississippi State, MS 39762, USA
[b] U.S. Department of Agriculture, Forest Service, Forest Products Laboratory, Madison, WI 53726, USA

ARTICLE INFO

Article history:
Received 4 March 2017
Received in revised form 9 May 2017
Accepted 28 May 2017
Available online 29 May 2017

Keywords:
Kraft lignin
Multi-layer graphene
Formation mechanism
Iron oxides nanoparticles
α-Fe nanoparticles

ABSTRACT

The formation of carbon-based nanomaterials was investigated through heating iron nitrate promoted kraft lignin at different temperatures up to 600 °C under argon gas at atmospheric pressure. High-resolution transmission electron microscopy and electron diffraction images showed that multi-layer turbostratic-structured graphene presented in samples heated at 600 °C. X-ray diffraction results indicated that iron oxides nanoparticles started their formation as an amorphous carbon matrix at 300 °C, and turned into α-Fe nanoparticles at 600 °C. It is believed that the formation of observed multi-layer graphene materials is based on the dissolution and precipitation mechanism of carbonaceous gases from lignin decomposition acting as carbon sources and α-Fe working as the catalyst.

1. Introduction

Lignin is the most abundant aromatic biopolymer on earth [1]. Each year, there are 70 million tons of lignin as a byproduct from the pulping industry worldwide [2]. However, most of the lignin, especially kraft lignin (80% of the world's chemical pulping lignin production [3]), is simply burned onsite for energy and cooking chemical recovery. Lignin contains more than 60% carbon and can be an alternative carbon source for carbon-based nanomaterials production. Carbon-based nanomaterials such as carbon nanotubes, graphene-encapsulated metal nanoparticles, and multi-layer graphene materials, etc. draw much attention from worldwide research groups because of their unique electric, magnetic, and mechanical properties. Recent research activities of using various solid carbon materials such as synthetic polymers [4], saccharides [5], and woody biomass [6–10] as carbon sources to synthesize carbon-based nanomaterials under metal catalysts of various forms such as metallic particles/films and metal salts. Scientists tend to use the dissolution and precipitation theory for interpretation of the formation of graphene materials from solid carbon materials when the metals having a high dissolution capacity of carbon such as iron and nickel are used as the catalyst [10–13]. But limited literature was found in investigating how solid carbon materials participate the formation of graphene materials, i.e., in the gas or solid forms during thermal decomposition of a biopolymer as the carbon source at the wider range of heating temperatures from 200 to 1000 °C when a metal salt is used as the catalyst source, and also the transformation process of the metal salt to metallic catalyst. In our recent study, the mixture of kraft lignin and iron nitrate nonahydrate was thermally treated at different temperature levels up to 1000 °C. The temperature effect on formation of carbon-based nanomaterials was investigated. This paper reported observations and findings from experiments performed at temperatures up to 600 °C.

2. Experimental

2.1. Materials

Kraft lignin supplied by Domtar Corp. (North Carolina) was used as a carbon source, which contained 97.1% lignin, 0.53% ash, and 1.7% sugar, and had a pH value of 6.2. Iron nitrate nonahydrate ($Fe(NO_3)_3\,9H_2O$, 98% purity), from Sigma-Aldrich, Inc., was used as the metal catalyst for the thermal treatment.

2.2. Precursor preparation

40 grams of kraft lignin were impregnated with 200 mL of iron nitrate solution (0.27 mol/L) to prepare the lignin-iron nitrate suspension. The weight ratio of iron to oven-dry lignin was 7.5%.

* Corresponding authors at: Forest Products Laboratory, One Gifford Pinchot Drive, Madison, WI 53726-2398, USA (Z. Cai). Department of Sustainable Bioproducts, Box 9820, Mississippi State, MS 39762-9820, USA (J. Zhang).
E-mail addresses: zcai@fs.fed.us (Z. Cai), jz27@msstate.edu (J. Zhang).

http://dx.doi.org/10.1016/j.matlet.2017.05.125
0167-577X/

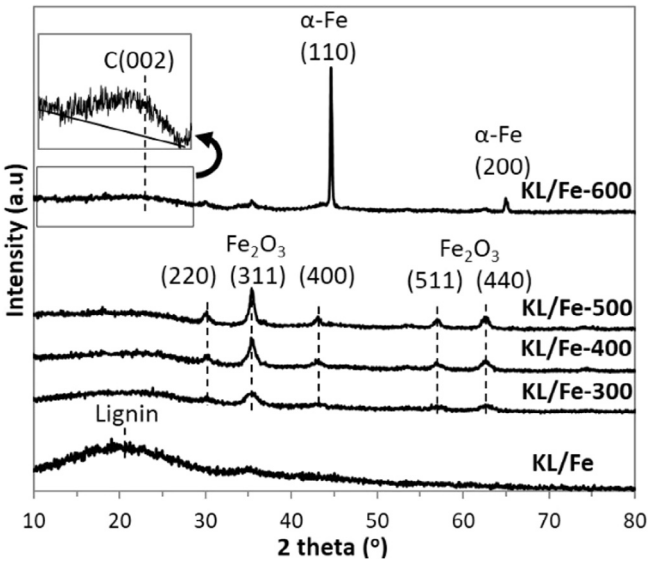

Fig. 1. XRD patterns of KL/Fe and KL/Fe-X samples.

The suspension was stirred in a 120 °C oil-bath for 0.5 h to evaporate water and obtain a sticky mixture, followed by drying the mixture for 2 h at 80 °C and then 48 h at 105 °C to obtain the dried precursor (KL/Fe).

2.3. Thermal treatment

The thermal treatment of KL/Fe samples was carried out in a split-hinge two-inch quartz tube electric furnace (Lindberg/BlueM1200) equipped with a temperature controller (Lindberg/BlueUTC150) under atmospheric pressure with an argon gas at a flow rate of 1.8 L/min. Four targeted temperature levels (300, 400, 500, 600 °C) were evaluated. For each run, four grams of KL/Fe samples were loaded into two porcelain boats (each holds 2 g) and inserted into the middle of the quartz tube. The thermal treatment started with argon gas (99.99%) flowing through the quartz tube for 15 min to remove oxygen from the system, followed by raising the temperature to a targeted level at a ramping rate of 20 °C/min. After holding each evaluated temperature for 1 h, the furnace was turned off. The sample was allowed to cool down naturally to room temperature, then removed out from the quartz tube, ground and labeled as KL/Fe-X, where X represents the evaluated temperature level, for instance, KL/Fe-300 represents the sample heated at 300 °C. In addition to the thermal treatment of KL/Fe samples using the described furnace system, the temperature-programmed decomposition-mass spectroscopy (TPD-MS) analysis of KL/Fe samples (5 g) was performed with the temperature raised from room temperature up to 600 °C at a ramping rate of 10 °C/min in a flowing nitrogen (99.99%, 150 mL/min) atmosphere at room pressure.

2.4. Characterization

X-ray diffraction (XRD) was performed on KL/Fe and KL/Fe-X samples with an Ultima3 diffractometer (CuKα radiation with λ = 1.5406 Å). The grain size of iron compounds in KL/Fe-X samples was calculated using Scherrer equation [14]:

$$L = \frac{0.9\lambda}{\sqrt{B_M^2 \quad B_S^2} \quad \cos\theta}$$

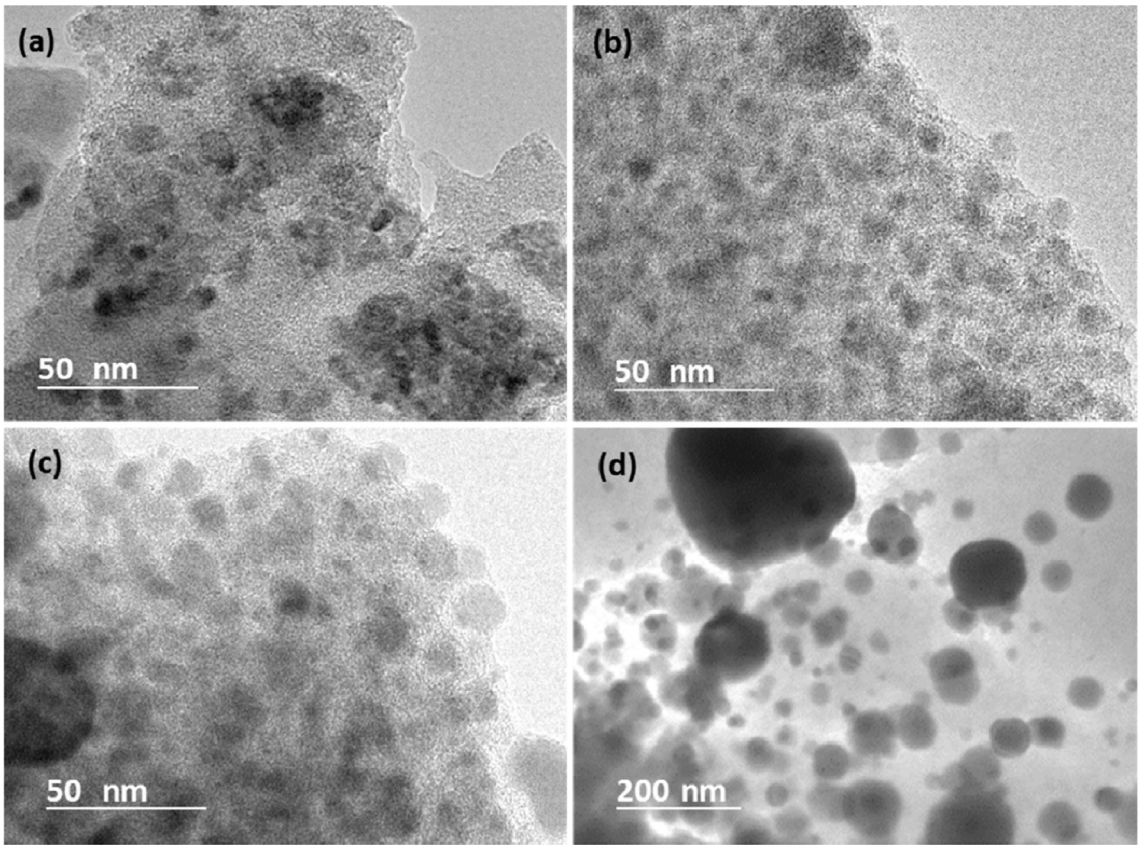

Fig. 2. Bright-field HRTEM images showing particles sizes of (a) KL/Fe-300, (b) KL/Fe-400, (c) KL/Fe-500, and (d) KL/Fe-600 samples, respectively.

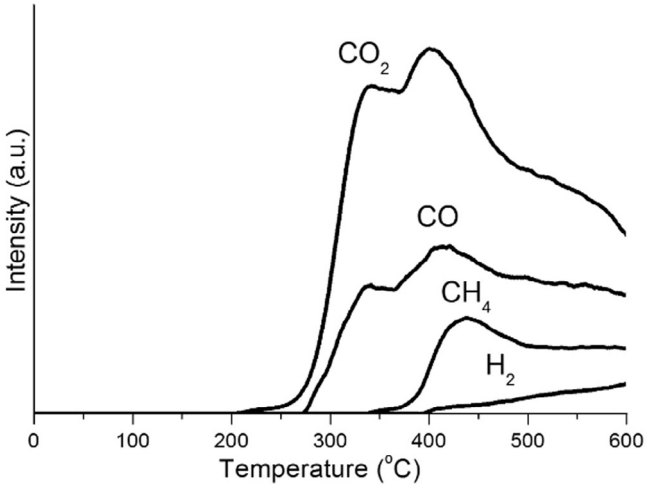

Fig. 3. Temperature-programmed decomposition-(TPD-MS) spectra of KL/Fe samples.

where λ is the wavelength of target CuKα (1.5406 Å), B_M is the full width at half maximum of the highest intensity diffracted plane, B_S is the full width at half maximum of standard materials in radians ($B_S = 0.1° \quad \pi/180°$), and θ is the peak angle for the highest intensity diffracted plane. High-resolution transmission electron microscopy (HRTEM) analysis of KL/Fe-X samples was performed on a JEM-2100 LaB6. The size distribution of nanoparticles observed on bright-field HRTEM images of KL/Fe-X samples was analyzed using the ImageJ software [15].

3. Results and discussion

Fig. 1 shows XRD patterns of KL/Fe and KL/Fe-X samples. The broad diffraction peak at $2\theta = 21°$ observed in KL/Fe samples indicates amorphous lignin structures [16]. There were no diffraction peaks related to iron phases observed in the KL/Fe samples. This suggested that iron ions could be chelated to lignin macromolecules [17]. Within a temperature range from 300 to 500 °C, the diffraction peaks at 30.1°, 35.4°, 43.1°, 57.0°, and 62.6° corresponded to (220), (311), (400), (511), and (440) reflections of iron oxides (Fe_2O_3) particles (Fig. 2) in KL/Fe-X samples, respectively [18,19]. The grain size of these Fe_2O_3 particles calculated using Scherrer equation was 5.4, 9.0, and 13.7 nm for temperatures 300, 400, and 500 °C, respectively. This size increase could be because neighboring iron oxide nanoparticles tended to agglomerate as the increasing temperature led further decomposition of lignin evidenced by TPD-MS spectra of KL/Fe (Fig. 3) showing more gases released from heated KL/Fe samples. As the temperature increased to 600 °C, the (110) and (200) plane diffraction peaks of body-centered cubic iron (α-Fe) were detected in KL/Fe-600 samples, indicating a reduction of Fe_2O_3 to iron particles. The calculated grain size of iron particles was 84.0 nm. The board and diffused peaks centered at $2\theta = 24°$ in KL/Fe-600 samples corresponding to the (002) reflection of carbon-based materials.

The HRTEM images (Fig. 2) show different sizes of nanoparticles (black spots) embedded in KL/Fe-X samples. The average diameters of these nanoparticles measured using ImageJ software were 5.68 (with its coefficient of variation of 14%), 8.91 (29%), 14.75 (23%) and 72.28 nm (49%) for 300, 400, 500, and 600 °C, respectively. These measurements were very close to grain sizes calculated based on XRD results. These nanoparticles embedded in amorphous carbon matrix had no layer graphene structure observed around nanoparticles in all KL/Fe-X samples (Fig. 2).

Multi-layer graphene (MLG) with its lateral size over one micrometer was observed only in KL/Fe-600 samples under HRTEM (Fig. 4a). The selected area diffraction (SAD) pattern (Fig. 4b) of measured MLG indicated a turbostratic stacking structure. Fig. 4c, a higher magnification image of the edge part of Fig. 4a as indicated with a bold arrow, shows MLG with the $d_{(002)}$ space of 3.50 nm, which was larger than the one of graphite ($d_{(002)} = 3.35$ Å). This further confirmed the turbostratic stacking structure of MLG observed in KL/Fe-600 samples.

The formation of MLG in KL/Fe-600 samples was believed to be through a chemical vapor deposition (CVD) process based on a dissolution and precipitation mechanism. In a typical CVD process, graphene materials are synthesized by running CH_4 or CO as carbon sources through transition metals such as iron at a minimum temperature of 600 °C [13,20,21]. The TPD-MS spectra of KL/Fe samples (Fig. 3) confirmed the existence of CH_4 and CO gases at 600 °C. The XRD result (Fig. 1) also indicated iron salt was completely converted to iron nanoparticles occurred at 600 °C. These gases as carbon sources and decompose at 600 °C can yield carbon atoms naked iron particles and form MLG. It is worth noting that the yield of MLG was very low because there was a very limited amount of naked iron particles distributed on the sample surface and most of the iron particles were trapped in amorphous carbon matrices (Fig. 2d).

4. Conclusions

This study revealed that iron ions in KL/Fe precursors started transitioning into Fe_2O_3 nanoparticles at 300 °C, and these

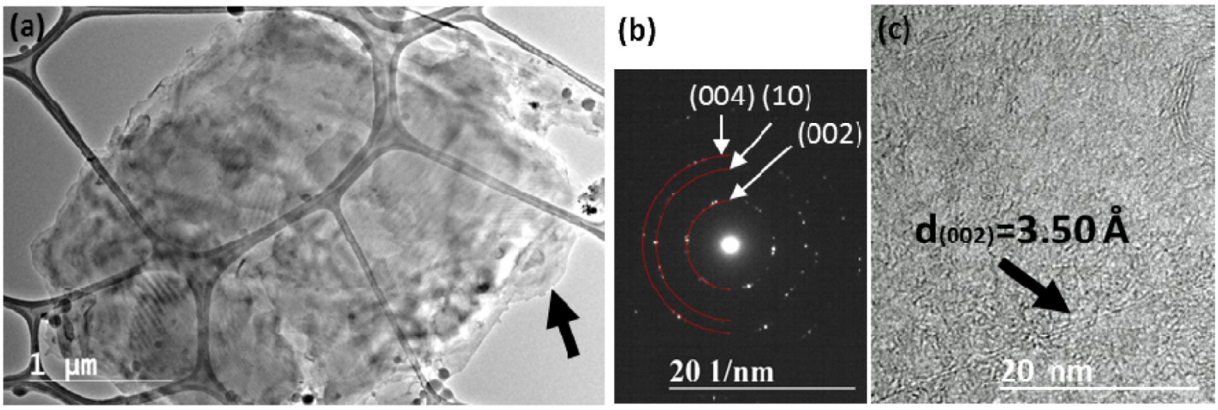

Fig. 4. Bright-field HRTEM images of (a) multi-layer graphene (MLG), (b) selected area diffraction (SAD) pattern of MLG edge as indicated by an arrow (a), and (c) bilayer graphene observed along arrow-indicated edge (a) in KL/Fe-600 samples.

nanoparticles tended to grow in grain size as the temperature kept increasing to 500 °C. At 600 °C, Fe_2O_3 nanoparticles were reduced to α-Fe nanoparticles embedded in amorphous carbon matrices. The formation of MLG in KL/Fe samples began as the temperature reached 600 °C. The formation mechanism is believed to be a CVD process.

Acknowledgements

This work was supported by the USDA Forest Service through Grant No. 16-JV-11111124-075. The authors would like to acknowledge Domtar Corp., North Carolina for providing kraft lignin for this study and Drs. Rooban Venkatesh K G Thirumalai and I-Wei Chu (Institute of Imaging and Analytical Technology, the Mississippi State University) for their assistance in characterization instruments. This manuscript is publication #SB894 of the Forest and Wildlife Research Center, Mississippi State University.

References

[1] M. Leisola, O. Pastinen, D.D. Axe, Lignin-designed randomness, BIO Complex. (2012).
[2] M.N. Satheesh Kumar, A.K. Mohanty, L. Erickson, M. Misra, Lignin and its applications with polymers, J. Biobased Mater. Bioenergy 3 (2009) 1–24.
[3] N. Mahmood, Z. Yuan, J. Schmidt, C. (Charles) Xu, Production of polyols via direct hydrolysis of kraft lignin: effect of process parameters, Bioresour. Technol. 139 (2013) 13–20.
[4] Z. Li, P. Wu, C. Wang, X. Fan, W. Zhang, X. Zhai, C. Zeng, Z. Li, J. Yang, J. Hou, Low-temperature growth of graphene by chemical vapor deposition using solid and liquid carbon sources, ACS Nano 5 (2011) 3385–3390.
[5] M. Sevilla, C. Sanchís, T. Valdés-Solís, E. Morallón, A.B. Fuertes, Direct synthesis of graphitic carbon nanostructures from saccharides and their use as electrocatalytic supports, Carbon 46 (2008) 931–939.
[6] S.P. Mun, Z. Cai, J. Zhang, Fe-catalyzed thermal conversion of sodium lignosulfonate to graphene, Mater. Lett. 100 (2013) 180–183.
[7] S.P. Mun, Z. Cai, J. Zhang, Preparation of Fe-cored carbon nanomaterials from mountain pine beetle-killed pine wood, Mater. Lett. 142 (2015) 45–48.
[8] M. Sevilla, C. Sanchís, T. Valdés-Solís, E. Morallón, A.B. Fuertes, Synthesis of graphitic carbon nanostructures from sawdust and their application as electrocatalyst supports, J. Phys. Chem. C 111 (2007) 9749–9756.
[9] W. Leng, H.M. Barnes, Q. Yan, Z. Cai, J. Zhang, Low temperature synthesis of graphene-encapsulated copper nanoparticles from kraft lignin, Mater. Lett. 185 (2016) 131–134.
[10] H. Zhao, T.S. Zhao, Graphene sheets fabricated from disposable paper cups as a catalyst support material for fuel cells, J. Mater. Chem. A 1 (2012) 183–187.
[11] H. Zhao, K.S. Hui, K.N. Hui, Synthesis of nitrogen-doped multilayer graphene from milk powder with melamine and their application to fuel cells, Carbon 76 (2014) 1–9, http://dx.doi.org/10.1016/j.carbon.2014.04.007.
[12] L. Baraton, Z.B. He, C.S. Lee, C.S. Cojocaru, M. Châtelet, J.-L. Maurice, Y.H. Lee, D. Pribat, On the mechanisms of precipitation of graphene on nickel thin films, EPL Europhys. Lett. 96 (2011) 46003.
[13] H. An, W.-J. Lee, J. Jung, Graphene synthesis on Fe foil using thermal CVD, Curr. Appl. Phys. 11 (2011) S81–S85.
[14] A. Monshi, M.R. Foroughi, M.R. Monshi, Modified Scherrer equation to estimate more accurately nano-crystallite size using XRD, World J. Nano Sci. Eng. 02 (2012) 154–160.
[15] X. Liu, M. Atwater, J. Wang, Q. Huo, Extinction coefficient of gold nanoparticles with different sizes and different capping ligands, Colloids Surf. B: Biointerfaces 58 (2007) 3–7.
[16] A. Goudarzi, L.-T. Lin, F.K. Ko, X-ray diffraction analysis of kraft lignins and lignin-derived carbon nanofibers, J. Nanotechnol. Eng. Med. 5 (2014), 021006 021006.
[17] S. Kubo, Y. Uraki, Y. Sano, Catalytic graphitization of hardwood acetic acid lignin with nickel acetate, J. Wood Sci. 49 (2003) 188–192.
[18] J.E. Lee, S.-H. Yu, D.J. Lee, D.-C. Lee, S.I. Han, Y.-E. Sung, T. Hyeon, Facile and economical synthesis of hierarchical carbon-coated magnetite nanocomposite particles and their applications in lithium ion battery anodes, Energy Environ. Sci. 5 (2012) 9528–9533.
[19] M. Fardis, A.P. Douvalis, D. Tsitrouli, I. Rabias, D. Stamopoulos, T. Kehagias, E. Karakosta, G. Diamantopoulos, T. Bakas, G. Papavassiliou, Structural, static and dynamic magnetic properties of dextran coated γ-Fe(2)O(3) nanoparticles studied by (57)Fe NMR, Mössbauer, TEM and magnetization measurements, J. Phys. Condens. Matter Inst. Phys. J. 24 (2012) 156001.
[20] M. Kumar, Y. Ando, Chemical vapor deposition of carbon nanotubes: a review on growth mechanism and mass production, J. Nanosci. Nanotechnol. 10 (2010) 3739–3758.
[21] J.-P. Tessonnier, D.S. Su, Recent progress on the growth mechanism of carbon nanotubes: a review, ChemSusChem 4 (2011) 824–847, http://dx.doi.org/10.1002/cssc.201100175.